ARTICLES

Hydrogen-Bonding Interactions of $(CF_3)_3CH$ and $(CF_3)_3C^-$ in the Gas Phase. An Experimental (FT-ICR) and Computational Study

Andrés Guerrero,[†] Rebeca Herrero,[†] Juan Z. Dávalos,[†] Ivar Koppel,[‡] José-Luis M. Abboud,*[,†] Antonio Chana,*[,†] and Ilmar A. Koppel*[,‡]

Instituto de Química Física Rocasolano, CSIC, C/Serrano 119, E-28006 Madrid, Spain, and Institute of Chemistry, Tartu University, Jakobi Street 2, 51014 Tartu, Estonia

Received: December 15, 2008; Revised Manuscript Received: April 15, 2009

Hydrogen-bonding interactions involving 2-(trifluoromethyl)-1,1,1,3,3,3-hexafluoropropane (**1**H) and $\mathbf{1}^-$ have been quantitatively studied by means of Fourier transform ion cyclotron resonance spectrometry. The existence of the species $(\mathbf{1}HCl)^-$ and $(\mathbf{1}H\mathbf{1})^-$ was demonstrated, and their thermodynamic stabilities were determined experimentally and computationally. In addition, some of their structural features were analyzed.

I. Introduction

We have been involved for some time in the study of the thermodynamic stability of 1:1 hydrogen-bonded complexes of neutral species, both in the gas phase[1] and in solution.[2] The stability of these complexes, formed by interaction of a neutral hydrogen-bond donor (A—H) and a hydrogen-bond acceptor (B), can be measured by the equilibrium constant K_p and/or the standard Gibbs energy change for reaction 1

$$AH(g) + B(g) \rightarrow AH\cdots B(g) \qquad K_{p(1)} \qquad \Delta_r G^0_m(1) \tag{1}$$

Numerous 1:1 complexes formed by a neutral molecule (A—H) and anions (B^-) in the gas phase

$$AH(g) + B^-(g) \rightarrow (AH\cdots B)(g) \qquad K_{p(2)} \qquad \Delta_r G^0_m(2) \tag{2}$$

have been studied by means of (i) mass-spectrometric techniques [notably Fourier transform ion cyclotron resonance spectrometry (FT-ICR)[3] and high-pressure mass spectrometry[4,5]], (ii) photodissociation spectroscopy,[6] (iii) electron photodetachment spectroscopy,[7] and (iv) multiphoton infrared dissociation spectra.[8] These anionic species include, among others, delocalized carbanions,[9] substituted acetylide ions,[10] and cyanide anion.[11] Intramolecular hydrogen bonds have been reported that also involve carbanionic centers.[12]

Reaction 2 has been observed in systems involving CH hydrogen-bond donors and several anions.[13]

It has been known for several decades[14] that, in solution, deprotonation of monohydrofluorocarbons (MHFs) of the general form C_nF_mH can lead to carbanions of the form $C_nF_m^-$. The possibility of determining their kinetic acidities using hydrogen/deuterium exchange was also established. This process was later used to compare the kinetic acidities of 2-(trifluoromethyl)-1,1,1,3,3,3-hexafluoropropane [or tris(trifluoromethyl)-methane C_4F_9H (**1**H)], 1*H*-perfluorobicyclo[2.2.2]octane (**2**H), and 1*H*-perfluorobicyclo[2.2.1] heptane (**3**H).[15]

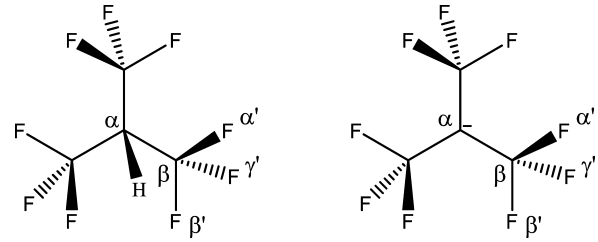

Figure 1. Chemical structures of C_4F_9H and $C_4F_9^-$. The nomenclature of the different nonequivalent atoms is also depicted.

The fact that the ranking of the rates of hydrogen/deuterium exchange is **1**H > **2**H ≫ **3**H was taken as an indication of the relevance of fluorine (negative) hyperconjugation. The hyperconjugative effect in $\mathbf{1}^-$ can be visualized as the contribution of the nine possible mesomeric structures shown in Figure 1. They ensure the dispersal of the negative charge over the fluorine atoms

$$C_4F_9^- \leftrightarrow C_4F_8F^-$$

Internal strain in $\mathbf{2}^-$ and particularly in $\mathbf{3}^-$ reduces this effect and, hence, explains the ranking of kinetic acidities.

The gas-phase acidity of an acid AH, GA, is measured by the standard Gibbs energy change for the reaction

$$HA(g) \rightarrow H^+(g) + A^-(g) \qquad GA = \Delta_r G^0_m(3) \tag{3}$$

Using FT-ICR spectrometry, we were able to show[16] that the ranking of *thermodynamic* acidities of **1**H, **2**H, and **3**H in the gas phase (process 3) is the same as found for their kinetic acidities in solution. This result, being "intrinsic" (solvent-independent), was taken as a strong argument in favor of the negative hyperconjugation of fluorine.

This work focuses on **1**H. This compound could act as a CH hydrogen-bond donor (HBD). Indeed, the complex between **1**H

* To whom correspondence should be addressed. E-mail: Jose Luis Abboud: jlabboud@iqfr.csic.es; Antonio Chana: achana@iqfr.csic.es; Ilmar Koppel: ilmar.koppel@ut.ee.
† Instituto de Química Física Rocasolano.
‡ Tartu University.

10.1021/jp811057m CCC: $40.75
Published on Web 05/19/2009

and DMSO in CCl_4 solution has been reported.[17] Also, the corresponding perfluorinated anion, *tert*-$C_4F_9^-$, is a potential hydrogen-bond acceptor (HBA).

For our present purposes, it is important that an FT-ICR study of the 1:1 complexes between fluoroform and various acetylides, $(F_3CH\cdots C'C-R)^-$, has shown that they have complexation energies of ca. 19 kcal mol^{-1}, substantially larger than those involved in ion−induced dipole complexes, and such species have thus been considered hydrogen-bonded complexes.[18] The existence and stability of more "classical" hydrogen-bonded complexes between F_3CH and alkoxide[19] and chloride[20] anions have also been determined. Furthermore, **1**H has a *GA* value of 326.6 ± 2.0 kcal mol^{-1}. This compound thus has an acidity close to those of HCl, $CF_3CH_2CO_2H$, and *p*-$CF_3C_6H_4CO_2H$ [328.1 (±0.2), 326.9 (±2.0), and 325.3 (±2.0) kcal mol^{-1}, respectively].[21] The hydrogen-bonding acidity of **1**H can be expected to be substantial, possibly higher than that of F_3CH.[22] Therefore, the determination of the HBD strength of **1**H seems of interest. As regards $\mathbf{1}^-$, important questions arise: (i) Does charge depletion of C(α) sufficiently reduce its hydrogen-bonding basicity to prevent its acting as a basic center? (ii) Do fluorine atoms carry enough charge to act as basic centers? The hydrogen-bonding basicity of monofluorinated hydrocarbons is rather small.[23] We present below an experimental and computational study aimed at answering these questions.

II. Experimental Section

II.1. Reagents. 1H is of the same batch as used in ref 16. The other compounds were obtained from Aldrich and were used without further purification. No significant amounts of impurities were detected in any case.

Caution: 1H can dehydrofluorinate to yield the highly toxic perfluoroisobutene. It should be handled with great care.

II.2. FT-ICR Spectrometer. In this work, use was made of a modified Bruker CMS-47 FT-ICR mass spectrometer. A detailed description of the original instrument is given in ref 24. It has been used in a number of recent studies.[25] Some salient features are as follows: The spectrometer is linked to an Omega Data Station (IonSpec, Lake Forest, CA). The high vacuum is provided by a Varian TURBO V550 turbomolecular pump (550 L s^{-1}). The magnetic field strength of the superconducting magnet is 4.7 T.

II.3. Experimental Techniques. Thoroughly degassed **1**H(g) (subjected to at least three pump-and-thaw cycles) was introduced into the high-vacuum section of the instrument. Typical partial pressures were in the range of $(3 \times 10^{-8})-(1 \times 10^{-6})$ mbar. The average temperature of the cell was ca. 321 K. *iso*-Amyl nitrite (*iso*-$C_5H_{11}NO_2$) containing ca. 20% methanol was added [nominal pressures of ca. $(2-4) \times 10^{-8}$ mbar]. Resonant capture of electrons provided a mixture of *iso*-amyl alkoxide and methoxide anions. After reaction times of less than 10 s, all *iso*-$C_5H_{11}O^-$ and CH_3O^- species were protonated by **1**H, thereby generating $\mathbf{1}^-$. In some experiments, a different acid, AH(g), was added to **1**H. It was treated as indicated above.

The readings of the Bayard-Alpert pressure gauge were corrected by means of the standard methods described in ref 25.

II.4. Computational Methods. In this work, we applied the hybrid density functional B3LYP[26] and MP2[27] ab initio techniques with basis sets ranging from 6-311+G(d,p) to 6-311++G(3df,2p).[28] In all cases, full geometry optimizations were performed, and computed the harmonic vibrational frequencies were calculated at the highest possible levels. Use was made of the Gaussian 03 package of computer programs.[29]

TABLE 1: Computed Values of *GA*(1H)[a,b]

level	*GA*
B3LYP/6-311+G(d,p)	319.2
B3LYP/6-311+G(3df,2p)	323.4
B3LYP/6/311++G(3df,2p)	323.3
MP2/6-311+G(d,p)	325.4
MP2/6-311++G(d,p)	325.6
MP2/6-311+G(3df,2p)	326.9
MP2/6-311++G(3df,2p)	326.3
experimental	326.6 ± 2.0[c]

[a] This work. [b] All values in kcal mol^{-1}. [c] From ref 21.

Natural bond orbital (NBO) calculations[30] were carried out using the package[31] included in Gaussian 03. Basis set superposition errors (BSSEs) are significant and were computed using the Boys−Bernardi method.[32b] Adducts were subjected to conformational searches, as a starting point for the quantum chemistry calculations. Sybyl 8.0 and the trypos force field were employed. Charges used for molecular dynamics were derived from the NBO analysis.

III. Experimental and Computational Results. Discussion

III.1. Gas-Phase Acidity and Structures of 1H and $\mathbf{1}^-$. 1. $\mathbf{1}^-$ has a significant thermodynamic stability. Indeed, its ^{19}F and ^{13}C NMR spectra in solution have been obtained,[32a] and its cesium salt proved to be a stable solid material.[33] This stability of $\mathbf{1}^-$ contributes to making **1**H(g) a strong acid, both in the gas phase and in solution.

Among the earlier computational studies,[33,34] a scaled PM3 method was applied to a vast set of Brønsted acids, including **1**H(g), in order to estimate their *GA* values. A more limited study followed, involving CF_3^-, $CF_3CH_2^-$, $CF_3CF_2^-$, $(CF_3)_2CF^-$, and $\mathbf{1}^-$. The latter study highlighted the importance of anionic hyperconjugation in the case of $\mathbf{1}^-$.[34] The experimental (electron diffraction) structure determination dates back to ref 35a. Recent experimental (microwave spectroscopy) and computational [MP2/6-311G(d,p) level] studies of the **1**H structure are due to Munrow et al. (see ref 35b). However, the computed acidity of **1**H was not reported in either of these works.

We summarize in Table 1 the computational *GA* values for **1**H obtained in this work.

The values obtained at the MP2 level are significantly closer to the experimental datum than those determined using DFT. We have reported a similar situation in a recent study on perfluorinated alcohols.[25c]

As generally occurs, the agreement between computed and experimental results rests in part on the cancellation of errors. Here, the MP2/6-311++G(3df,2p) level seems reasonably satisfactory for **1**H. The results are somewhat less so when HCl is considered. Thus, in the range of acidities involved in this study, the calculated [MP2/6-311++G(3df,2p)] *GA* for HCl is 326.1 kcal mol^{-1}. At the CCSD/6-311++G(3df,2p) level, the computed value of *GA*(HCl) is 328.6 kcal mol^{-1}, in better agreement with the most accurate experimental value available, 328.1 ± 0.2 kcal mol^{-1}.[21] Computations at this level with heavier species are too time-consuming for our computational means. Therefore, whenever possible, we used processes in which cancellation of errors is easier.

The structures of **1**H (point group C_3) and $\mathbf{1}^-$ (point group C_3) optimized at the MP2/6-311++G(3df,2p) level are presented in Figure 1. The various bond lengths and bond angles are summarized in Table 2. To our knowledge, no experimental data are available on the structure of $\mathbf{1}^-$. Electron diffraction data for **1**H[35a] are given in Table 2.

TABLE 2: Computed [MP2/6-311++G(3df,2p)] and Experimental[a] Bond Lengths[b] and Bond Angles[c] for 1H and 1^-

	C_4F_9H (C_3)	$C_4F_9^-$ (C_3)	$C_4F_9^-$ (C_{3h})
C(α)—C(β)	1.531(1.537)	1.448	1.445
C(β)—F(α′)	1.333(1.334)	1.351	1.352
C(β)—F(β′)	1.332(1.334)	1.368	1.375
C(β)—F(γ′)	1.330(1.334)	1.380	—
C(β)C(α)C(β)	111.70(112.90)	118.81	120.00
C(α)C(β)F(α′)	110.09(110.90)	111.57	111.46
C(α)C(β)F(β′)	110.74(110.90)	115.23	115.76
C(α)C(β)F(γ′)	111.81(110.90)	116.06	—
F(α′)C(β)F(β′)	107.58(108.00)	105.60	105.22
F(α′)C(β)F(γ′)	108.30(108.00)	104.79	—
F(β′)C(β)F(γ′)	108.20(108.00)	102.42	—
HC(α)C(β)	107.14(105.80)	—	—

[a] Experimental values taken from ref 35a. [b] In angstroms. [c] In degrees.

For the geometry of **1**H,[35a] the agreement between the experimental and computational data for bond lengths (better than 0.01 Å) and bond angles (ca. 1°) is rather satisfactory.

To our knowledge, no experimental information is available on the structure of $\mathbf{1}^-$. Geometry optimizations using various DFT levels [B3LYP/6-311+G(d,p) and B3LYP/6/311+G(3df,2p)] and MP2/6-311+G(d,p), yield a C_{3h} symmetry for this ion, all the computed vibrational frequencies being real. In this structure, C(α) is in the plane of the three β carbons. The lowest harmonic vibrational frequency corresponds to the "out-of-plane" (plane defined by the three β carbons) motion of C(α) leading to the inversion of the α carbon. However, optimization at the MP2/6-311+G(3df,2p) level indicates that the structure of $\mathbf{1}^-$ is of C_3 symmetry (see Figure 1), slightly pyramidalized, with C(α) being 0.16 Å from the plane defined by the three β carbons (this distance amounts to 0.45 Å in **1**H). All of the harmonic vibrational frequencies are real, corresponding to a minimum on the potential energy surface (PES) of $\mathbf{1}^-$. This, together with the small difference in standard Gibbs free energy between the C_3 (minimum) and C_{3h} (transition-state) structures, 1.76 kcal mol^{-1}, suggests again that the "inversion" of the α carbon takes place at room temperature. The lowest vibrational mode of $\mathbf{1}^-$ (32.9 cm^{-1}) is associated with the symmetrical stretching of the α carbon with respect to the three β carbons. The imaginary vibrational frequency (26.9i cm^{-1}) corresponds to the out-of-plane (defined by the three β carbons) vibration leading to the inversion of the α carbon. Relevant structural features of the C_3 structure as optimized at the MP2/6-311+G(3df, 2p) level are as follows: (i) The C(α)—C(β), distance, 1.448 Å is substantially shorter than that found in **1**H (1.537 Å), and this is quite consistent with the hyperconjugative effect indicated above. (ii) The C(β)—F(γ′), C(β)—F(β′), and C(β)—F(α′) bond lengths, 1.380, 1.368, and 1.351 Å, respectively, correspond to C—F bonds in antiperiplanar and synperiplanar (in the latter two cases) orientations with respect to the C(α)—lone pair orbital. Again, this is to be expected on the basis of fluorine hyperconjugation.

TABLE 3: Natural Charges[a,b] for the Atoms of 1H and 1^- (C_3)

1H (C_3)		$\mathbf{1}^-$ (C_3)	
atom	charge	atom	charge
C(α)	−0.437	C(α)	−0.767
C(β)	1.207	C(β)	1.236
F(α′)	−0.384	F(α′)	−0.423
F(β′)	−0.383	F(β′)	−0.439
F(γ′)	−0.380	F(γ′)	−0.452
H	0.255		

[a] In electronic charge units. [b] 6-311++G(3df,2p) basis set and geometry optimized at the MP2/6-311++G(3df,2p) level.

2. An NBO study at the MP2/6-311++G(3df,2p) level was carried out for both species. The corresponding charges on the atoms of both species are summarized in Table 3.

The computed positive charge on the hydrogen atom of **1**H, 0.255, is significantly larger than that on the hydrogen of fluoroform (0.087, this work). The patterns of charge distributions in **1**H and $\mathbf{1}^-$ are rather similar. In the latter case, however, the negative charge on C(α) is ca. 0.3 electronic units larger than in the former. Interestingly, the negative charges on the various F atoms increase by a small amount, 0.03−0.06 electronic units, on going from **1**H to $\mathbf{1}^-$. The fact that the electronic population ranks as F(α′) < F(β′) < F(γ′) is consistent with the previous discussion on hyperconjugation effects.

The highest occupied molecular orbital (HOMO) of $\mathbf{1}^-$ involves a large contribution from the p_z orbital of C(α) and significantly smaller contributions from the three p_z orbitals of C(β). The p orbitals of the F atoms are involved in lower-lying orbitals and are, therefore, less prone to act as basic centers.

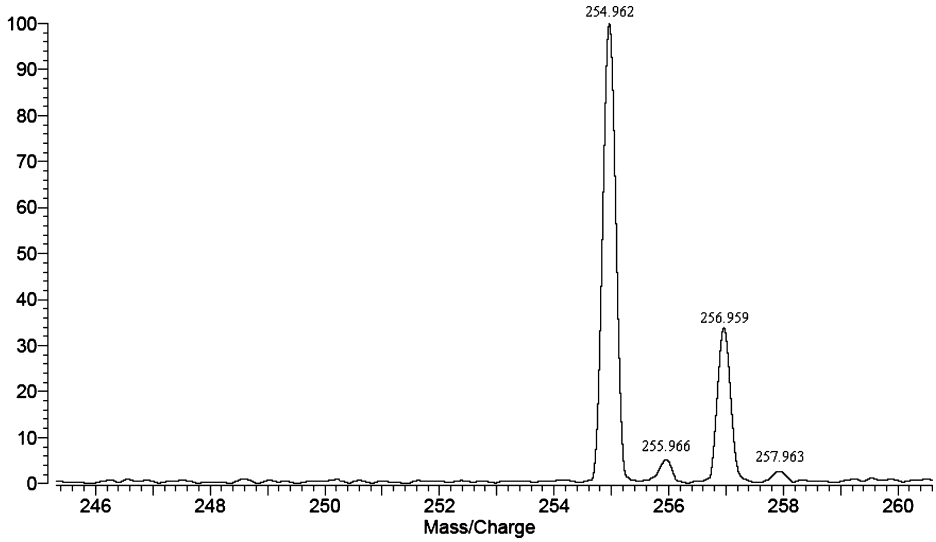

Figure 2. Mass spectrum of ion $(\mathbf{1}HCl)^-$ (pressure of **1**H, 9.6×10^{-7} mbar; pressure of HCl, 1.2×10^{-7} mbar; 50 scans).

We have also determined the Wiberg indexes[36] of $\mathbf{1}^-$. For C(α)—C(β), we found 1.10. For C(β)—F(γ′), C(β)—F(β′), and C(β)—F(α′), values of 0.775, 0.795, and 0.825, respectively, were obtained. These values are quite consistent with the charge distribution indicated above and with the hyperconjugative effect of fluorine, The hyperconjugative effect is stereoelectronic, and consequently, when the bond C—F is in an antiperiplanar arrangement with respect to the lone pair in C(α), the maximum values are observed.

III.2. 1:1 Hydrogen-Bonded Complexes. One could expect that the anions A^- of protic acids with acidities significantly weaker than that of **1**H would be practically fully protonated by **1**H and that the opposite would occur with acids significantly stronger than **1**H. We have explored a series of systems including **1**H and a variety of acids AH with *GA* values spanning the range from 383.7 ± 0.2 (H_2O) to 315.4 ± 2.0 ($MeSO_3H$).[21] With only two exceptions, we never observed any significant amount of hydrogen-bonded adducts, $(\mathbf{1}HA)^-$. These exceptions are discussed in the following subsections.

***III.2.1. (1HCl)*$^-$.** The mass spectrum of this ion is presented in Figure 2. In the gas phase, *GA*(HCl) = 328.1 ± 0.2 kcal mol^{-1} and *GA*(**1**H) = 326.6 ± 2.0 kcal mol^{-1}.Thus, under pressures of HCl and **1**H of the same order of magnitude, both Cl^- and $\mathbf{1}^-$ coexist in the presence of their corresponding neutral acids and their hydrogen-bonded adducts. This point was confirmed by double-resonance experiments. Pressures of HCl and **1**H were in the range from 2.0×10^{-8} to 1.0×10^{-6} mbar.

Collision-induced decomposition of $(\mathbf{1}HCl)^-$ using Ar as the collision gas cleanly leads to the formation of $\mathbf{1}^-$, without any significant amount of Cl^-. This, however, is not a proof of the ion structure being $(Cl—H\cdots\mathbf{1})^-$.

In this work, we observed the equilibria

$$Cl^- + HCl \rightarrow (ClHCl)^- \qquad K_p(4) \qquad \Delta_r G^0_m(4) \quad (4)$$

$$(ClHCl)^- + \mathbf{1}H \rightarrow (\mathbf{1}HCl)^- + HCl \qquad K_p(6) \qquad \Delta_r G^0_m(5) \quad (5)$$

(supported in all cases by double-resonance experiments).

Reaction 5 leads to the expression

$$K_p(6) = \left[\frac{I_{(\mathbf{1}HCl)^-}}{I_{(ClHCl)^-}}\right] \times \left[\frac{P_{HCl}}{P_{\mathbf{1}H}}\right] \quad (6)$$

In these and the following expressions, the *P* variables represent the partial pressures of the neutral species, and the *I* variables represent the abundances of the various ions (corrected for the relative abundances of their isotopologs and taken as directly proportional to their partial pressures).

Equation 5 allows the direct comparison of the thermodynamic stabilities of $(\mathbf{1}HCl)^-$ and $(ClHCl)^-$. Ion selection experiments show that, in every case, the ratio $[I_{(\mathbf{1}HCl)^-}/I_{(ClHCl)^-}]$ reaches a constant value independent (within 10% or better) of the ion being selected. A plot of this ratio against the ratio $P_{\mathbf{1}H}/P_{HCl}$ is linear (see Figure 3), and with the appropriate corrections, its slope provides the value of $K_p(5)$. The experimental results are summarized in Table 4.

Combination of $\Delta_r G^0_m(4)$ and $\Delta_r G^0_m(5)$ leads to a value for $\Delta_r G^0_m(7)$ based solely on experimental data. $\Delta_r G^0_m(7)$ pertains to the reaction

$$\mathbf{1}H + Cl^- \rightarrow (\mathbf{1}HCl)^- \qquad \Delta_r G^0_m(7) \quad (7)$$

Reactions 7 and 5 were thus subjected to a computational study. The results are also summarized in Table 4. Consideration of the result obtained for reaction 4 strongly suggests that basis set superposition error (BSSE) is important in the calculations carried out at the MP2/6-311++G(3df,2p) level. We have thus applied the Boys—Bernardi correction[32a] to the adducts $(ClHCl)^-$ and $(\mathbf{1}HCl)^-$. The results are given in Table 4. In the case of $(\mathbf{1}HCl)^-$, we considered the moieties (Cl^-, **1**H) (italicized results) and (HCl, $\mathbf{1}^-$). The agreement between the computed and experimental results is rather good for the former treatment.

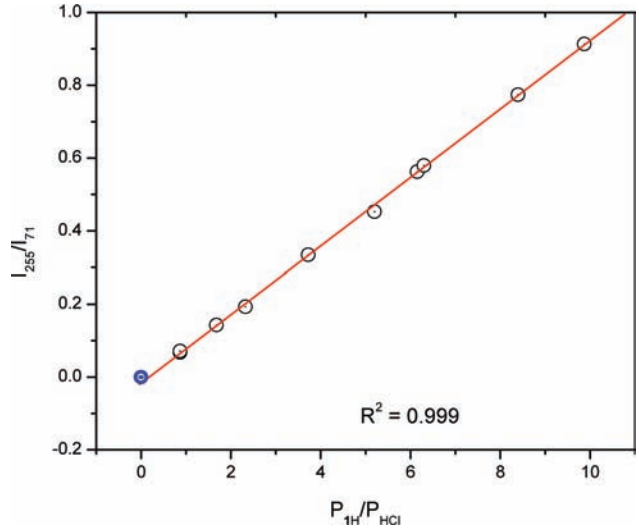

Figure 3. Plot of the ratio of ion intensitites (I_{255}/I_{71}) against the (uncorrected) ratio of the partial pressures (P_{1H}/P_{HCl}). In blue is the (0,0) point, not included in the correlation.

The optimized structure of $(\mathbf{1}HCl)^-$ at the MP2/6-311++G(3df,2p) level is shown in Figure 5 below. Relevant bond distances are summarized in Table 5. They tend to indicate that this complex can be seen as a neutral **1**H moiety hydrogen-bonded to a chloride anion.

***III.2.2. (1H1)*$^-$.** Using relatively high pressures of **1**H [on the order of $(1-2) \times 10^{-6}$ mbar] and no cooling gas, we observed the formation of the ion with m/z = 439 and its isotopologs, corresponding to the $(\mathbf{1}H\mathbf{1})^-$ ion (see Figure 4). The abundance of this species is rather small (2−3% of that of **1**H), and most important, the ion disappears in a few seconds. It seems reasonable to infer that this ion is formed by the reaction between **1**H and excited $\mathbf{1}^-$. The excitation of the anion would originate in the energy released by the reaction between **1**H and the alkoxides MeO^- and *iso*-AmO^-. If the standard Gibbs energy change for reaction 8 is too weakly negative or even slightly positive, $(\mathbf{1}H\mathbf{1})^-$ is expected to dissociate as it thermalizes through collisions with the neutral species present in the system.

$$\mathbf{1}H + \mathbf{1}^- \rightarrow (\mathbf{1}H\mathbf{1})^- \qquad \Delta_r G^0_m(8) \quad (8)$$

A problem to take into account is the conformations that the two interacting species can adopt. This is not a trivial problem, as the conformational space of two interacting compounds can be vast. We have searched for possible interaction conformations by means of the simulated annealing[37] molecular dynamics method. It allows searching possible minima with molecular dynamics in systems, such as the present one, where systematic searches are forbidden given the degrees of freedom for noncovalently bonded molecules.

In that way, we produced two initial conformations (**sI** and **sII**, Figure 5) derived by chemical "intuition". Thus, we assumed that the hydrogen atom in **1**H would tend to approach the sites with the largest negative charges in $\mathbf{1}^-$, namely, C(α) and the fluorine atoms. **sI** and **sII** were afterward recursively heated

TABLE 4: Experimental and Computational Standard Gibbs Energy Changes Pertaining to Relevant Processes[a]

reaction	level	uncorrected[b]	BSSE-corrected[b,c]	experiment
$Cl^- + HCl \rightarrow (ClHCl)^-$	MP2/6-311++G**	−17.6	*−13.0*	−16.5 ± 0.3[d]
	MP2/6-311++G(3df,2p)	−18.6	*−16.5*	
$\mathbf{1}H + Cl^- \rightarrow (\mathbf{1}HCl)^-$	MP2/6-311++G**	−20.1	*−13.7*	−15.5 ± 0.3[b]
			−11.5	
	MP2/6-311++G(3df,2p)	−17.3	*−15.0*	
			−13.6	
$(ClHCl)^- + \mathbf{1}H \rightarrow (\mathbf{1}HCl)^- + HCl$	MP2/6-311++G**	−2.6	*−0.75*	1.0 ± 0.2[b]
			1.46	
	MP2/6-311++G(3df,2p)	1.3	*1.5*	
			2.9	

[a] All values in kcal mol^{-1}. [b] This work. [c] See text. Italiziced values correspond to the effect of the Cl^- moiety. [d] From ref 21.

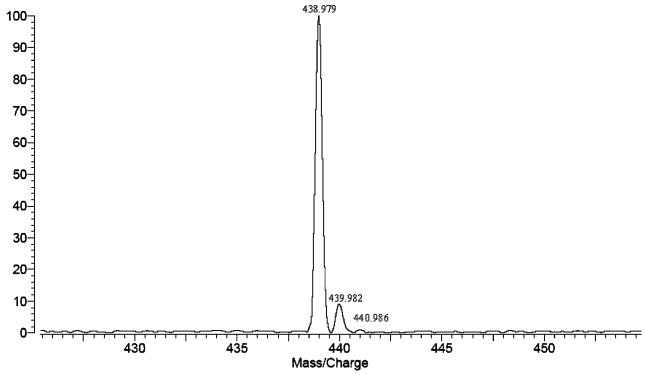

Figure 4. Spectrum of $(\mathbf{1}H\mathbf{1})^-$. Detection time = 300 ms after ionization. $P_{1H} = 1.02 \times 10^{-6}$ mbar. 100 transients.

TABLE 5: Computed Bond Distances Pertaining to $(1HCl)^-$ and HCl[a,b]

species	d[C(α)—H]	d(H—Cl)
$(C_4F_9HCl)^-$	1.133	2.019
C_4F_9H	1.090	—
HCl	—	1.273

[a] MP2/6-311++G(3df,2p) level. [b] All values in angstroms.

and cooled for 100 times each to find the corresponding conformational minima. Such minima were finally minimized and analyzed by molecular mechanics methods. This led to three possible conformations: **mI**, **mII**, and **mIII** (see Figure 5).

These conformations were optimized at the B3LYP/6-311++G(3df,2p) level, leading, during the optimization process, to the conformations **Ia**, **Ib**, and **II** used for this study. Some relevant interatomic distances are given in Table 6. The energy levels of these minima are rather close; indeed, the difference between **Ia** and **Ib** is around 0.1 kcal/mol, and **II** is 1.5 kcal mol^{-1} higher. All of them are true minima, as confirmed by frequency analysis.

In **Ia**, the "bond" between H and the negatively charged C(α) is long, 2.403 Å, whereas in **Ib**, the length is slightly shorter, 2.377 Å. This is likely a consequence of the repulsion between the C—F dipoles in the two moieties. Indeed, these bonds are in eclipsed positions in **Ia**, whereas in **Ib**, they are staggered, thus minimizing the repulsive interactions. In **II**, the H—F(β') and H—F(γ') distances are also long and very similar. This suggests an essentially electrostatic interaction in both cases. The calculations at the B3LYP/6-311++G(3df,2p) lead to the standard enthalpy and Gibbs energy changes for the formation of structures **Ia**, **Ib**, and **II** reported in Table 7. In terms of the computed $\Delta_r G^0_m(8)$ values, the structures **Ia**, **Ib** and **II** are very similar, and at sufficiently high pressures, the three species should coexist. Of course, at the low pressures prevailing in the experiments, the equilibrium concentrations of these species are vanishingly small, in agreement with our observations.

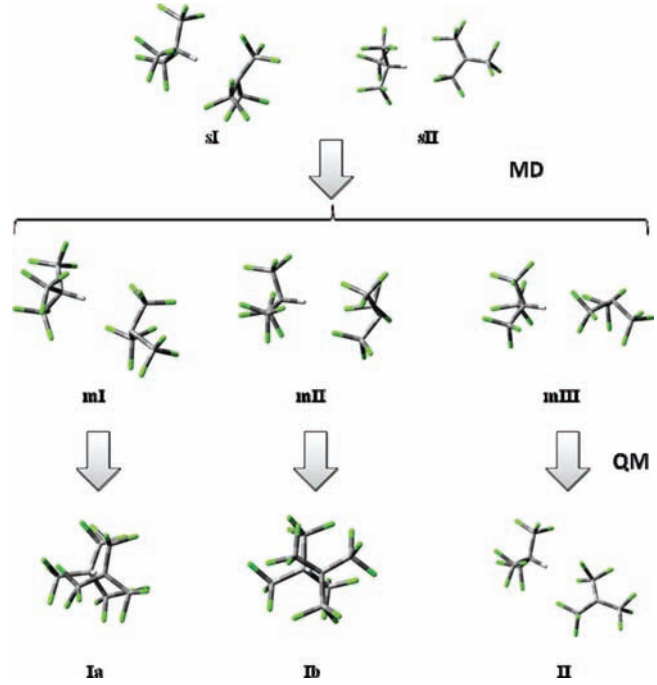

Figure 5. Starting geometries for the MM conformational search and QM-optimized [B3LYP/6-311++G(3df,2p) level] adduct conformations.

TABLE 6: Computed Bond Lengths for $C_4F_9H—C_4F_9^-$ [a,b]

distance	$C_4F_9H—C_4F_9^-$ **Ia** (C_3)	$C_4F_9H—C_4F_9^-$ **Ib** (C_1)	$C_4F_9H—C_4F_9^-$ **II** (C_1)
C(α,1)—H /C(α,2)—H	1.109	1.109	1.094
C(α,1′)—H/C(α,2′)—H	2.403	2.377	3.765
H—F(α′)	3.472	3.45	3.931
H—F(β')	2.929	2.902	2.343
H—F(γ')	4.352	4.323	2.319

[a] B3LYP/6-311++G(3df,2p) level. [b] All values in angstroms.

TABLE 7: Calculated Thermodynamic Data for Reaction 8[a,b]

property	**Ia** (C_3)	**Ib**	**II** (C_1)
$\Delta_r G^0_m(8)$	0.5	0.9	−0.8
$\Delta_r H^0_m(8)$	−10.0	−10.8	−8.9

[a] B3LYP/6-311++G(3df,2p) level. [b] All values in kcal mol^{-1}.

An NBO study, at the B3LYP/6-311++G(3df,2p) level, was carried out in order to understand the orbital interactions within the complex species. More precisely, we studied $C_4F_9HCl^-$ and the structures **Ia**, **Ib**, and **II** of $\mathbf{1}H\mathbf{1}^-$. NBO analysis was

TABLE 8: Results of the AIM Study of Relevant Species

species	bond	ρ_b	$\nabla^2\rho_b$	BL[a,b]	vdW radii[b]	
$(C_4F_9HCl)^-$	H···Cl	0.040	0.08	2.018	H, 1.02	Cl^-, 1.89
	C−H	0.271	−1.06	1.13	H, 1.02	C, 1.70
$(Cl···H···Cl)^-$	H···Cl	0.119	−0.15	1.253	H, 1.02	Cl^-, 1.89
$(C_4F_9HC_4F_9)^-$ Ia	H···C^-	0.016	0.033	2.4	H, 1.02	C^-, 1.68
	C−H	0.279	−1.04	1.108	H, 1.02	C, 1.70
$(C_4F_9HC_4F_9)^-$ Ib	H···C^-	0.017	0.035	2.37	H, 1.02	C^- 1.68
	C−H	0.273	−0.924	1.109	H, 1.02	C, 1.70
$(C_4F_9HC_4F_9)^-$ II	H···F(β')	0.012	0.044	2.318	H, 1.02	F, 1.47
	H···F(γ')	0.008	0.032	2.59	H, 1.02	F, 1.47

[a] Bond lengths. [b] In angstroms.

performed using NBO version 3.1 for Gaussian 03. In all species, the natural charges placed on the central carbon are rather similar to that observed within the single species already noted in section II. Indeed, the observed effect, the carbon linked to H does not present a lone pair of electrons whereas the anion does, its electronic configuration is quite close to it, indicating the weakness of this bond increased by the effect from the anionic side.

The second-order perturbation theory analysis exhibits some remarkable characteristics. The antibonding orbital between carbon and hydrogen receives charge from the central carbon in the anion, stabilizing the molecule by around 7.70 kcal mol^{-1} for **Ia** and 8.23 kcal mol^{-1} for **Ib**. Such an effect is also observed for the F—H interactions, where it is possible to see some donor−acceptor effect with the lone pairs of the F involved (see Bader analysis) although the largest contribution to the molecular stability is only 2.42 kcal mol^{-1}, indicating the greater stabilizing effect of the adduct than the H···F hydrogen bonds. This effect is obviously higher when chlorine anion is involved, contributing with one of its lone pairs to 35.42 kcal mol^{-1} of adduct stabilization.

III.2.3. Atoms in Molecules Analyses. Using Bader theory,[39] we can analyze the bond character when some sort of interaction can be found between two nuclei. There are several methods for performing this analysis, but a very intuitive one consists of checking two parameters: the electronic density at the bond critical point (ρ_b) and the Laplacian of the electronic density ($\nabla^2\rho_b$).The larger ρ_b, the more charge density is enclosed between the atoms. The sign of the Laplacian indicates whether the electronic density is concentrated, such as in covalent bonds, where $\nabla^2\rho_b < 0$, or depleted, such as in electrostatic interactions, where $\nabla^2\rho_b > 0$.[40]

The results of this study, using the structures optimized at the MP2/6-311++G(3df, 2p) level and wave functions generated at the B3LYP/6-311++G(3df,2p) level, are summarized in Table 8.

The study of the interaction between C_4F_9H and Cl^- leads to the system graph shown in Figure 6.

The values given for the H···Cl interaction in Table 8 (ρ_b = 0.040 and $\nabla^2\rho_b$ = 0.08,) are usually found in closed-shell interactions, which is therefore in agreement with an electrostatic interaction. On the other hand, the C—H bond shows values (ρ_b = 0.2715 $\nabla^2\rho_b$ = −1.06) consistent with a covalent bond.

When the same treatment is carried out for $(ClHCl)^-$, we find that the two H···Cl bonds are completely symmetrical, with ρ_b and $\nabla^2\rho_b$ showing some covalent character, although both the charge density and the Laplacian exhibit low absolute values, close to the frontier between covalent and ionic interactions. The H···Cl bond distances are identical and in the range of covalent bonds. Actually, this structure (a four-electron three-center bond) can be considered as the equilibrium state where the hydrogen atom, through the stretching vibration, is shifting from an electrostatic interaction to a covalent bond from one end to the other but, because the molecular symmetry, the observable is the average of the extreme structures. This is fully consistent with very thorough studies of this ion.[41,42]

It is possible as well to estimate the strength of the electrostatic interaction by determining the overlapping of the van der Waals (vdW) radii of the species,[43] measuring the distance from the nucleus of the selected atom within the intersection of the topological path at ρ_b = 0.001 for the isolated chemical species, in this case, Cl^-, C_4F_9H, and HCl. Although there are more sophisticated methods for this task,[44] such calculations can be easily performed using the electronic density cube files provided by Gaussian for the individual species, interpolating the selected electronic density for the vdW density along the bond direction. In that way, the more overlapped the radii are, the stronger the interaction is. The bond lengths and vdW radii given in Table 8 indicate that there is a clear overlap of the vdW surfaces in the case of $(\mathbf{1}HCl)^-$, but it is still too small for this bond to be considered covalent.

In the case of structures **Ia** and **Ib** (see Figure 7) for the adducts, the ρ_b and $\nabla^2\rho_b$ values for the critical point between H and C^- correspond to an electrostatic interaction, whereas that between C and H in the C_4F_9H moiety seems clearly associated with a covalent bond.

The H···C^- distances in adducts **Ia** and **Ib** are rather long, but given the conformational strain associated with such structures and the results of the Bader analysis, we can consider

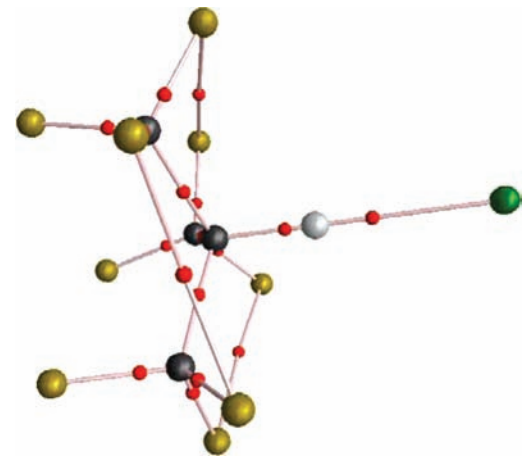

Figure 6. Molecular graph showing the bond critical points (red dots) and bond paths (white lines) in the $(C_4F_9HCl)^-$ structure optimized at the B3LYP/6-311++G(3df,2p) level.

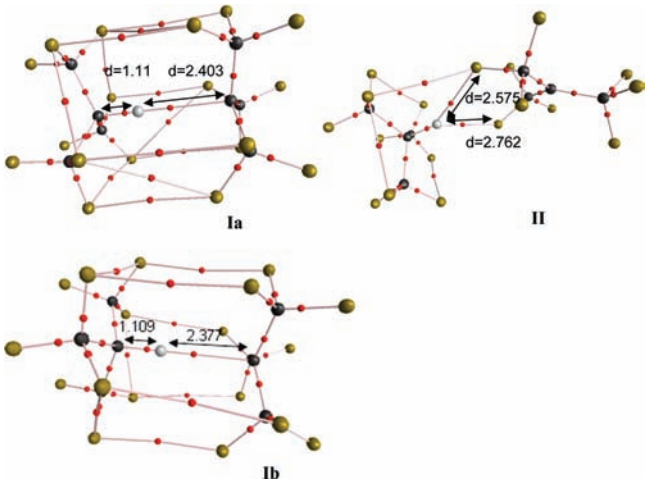

Figure 7. Molecular graph for structures**Ia**, **Ib**, and **II** of $(1H1)^-$ optimized at the B3LYP/6-311++G(3df,2p) level. Red dots are bond critical points, and white lines are bond paths.

them to be typical hydrogen bonds. In the case of **II**, the data in Table 8 suggest that the individual H···F interactions can be considered as rather weak. These results are also confirmed by the frequency analysis carried out for this dimeric species because its vibrational frequencies do not seem to be significantly influenced by the interaction with the hydrogen atom.

From a chemical point of view, the presence of a critical point between fluorine atoms is surprising, yet it can be considered as a simple overlap of charge densities surrounding the fluorine nuclei. As a consequence, in the analysis of the charge density, a nonzero value is found, and therefore, the AIM analysis identifies it as a critical point. Does this fact mean that it is a chemical interaction of any sort? When we analyze ρ_b or $\nabla^2\rho_b$, we find values of around 1×10^{-2}, quite low indeed, although not without precedent both in absolute values and in distances.[45] Even the eigenvalues (curvatures), the two negative and the positive one, present absolute values ranging from 1×10^{-3} to 1×10^{-2}, showing that, although such an effect indicates a concentration of charge density at the critical point, it is rather low and combined with a closed-shell interaction. Such types of interactions have been associated with molecules containing either fluorine or oxygen atoms in close contact.[46,47] The second-order perturbation theory performed within the NBO analysis for such interactions shows a low (around 0.1 kcal mol^{-1} in average), although not nil, contribution to the stability of the molecule. Here, the lone pairs of the closest fluorine atoms donate their electronic pairs to the extravalence orbitals of neighbor fluorine atoms, resulting in a net increase of the adduct stability, and therefore, such interactions, as described by means of AIM theory, are perfectly consistent with systems with such internal repulsion.

Acknowledgment. This study was supported by Grant CTQ2006-10178/BQU from the Spanish MEyC, Grant 6701 from the Estonian Science Foundation, and a CSIC−Estonian Academy of Science joint project. Work by A.C. was carried out under a JAE contract with CSIC.

Supporting Information Available: Optimized coordinates of all chemical species calculated at the MP2/6-311++G(3df,2p) theoretical level. This material is available free of charge via the Internet at http://pubs.acs.org.

References and Notes

(1) Marco, J.; Orza, J. M.; Notario, R.; Abboud, J.-L. M. *J. Am. Chem. Soc.* **1994**, *116*, 8841–8842.

(2) (a) Abboud, J.-L. M.; Sraïdi, K.; Negro, A.; Kamlet, M. J.; Taft, R. W. *J. Org. Chem.* **1985**, *50*, 2870–2873. (b) Frange, B.; Abboud, J.-L. M.; Benamou, C.; Bellon, L. *J. Org. Chem.* **1982**, *47*, 4553–4557. (c) Bellon, L; Taft, R. W.; Abboud, J.-L. M. *J. Org. Chem.* **1980**, *45*, 1166–168. (d) Abboud, J.-L. M.; Bellon, L. *Ann. Chim. (Paris)* **1970**, *5*, 63–74.

(3) (a) Marshall, A. G.; C, L; Hendrickson, C. L. *Int. J. Mass Spectrom.* **2002**, *215*, 59. (b) Gal, J.-F.; Maria, P.-C.; Raczynska, E. W. *J. Mass. Spectrom.* **2001**, *36*, 699. (c) Abboud, J.-L. M.; Notario, R. In *Energetics of Stable Molecules and Reactive Intermediates*; Minas da Piedade, M. E., Ed.; NATO Science Series C; Kluwer: Dordrecht, The Netherlands, 1999; Vol. 535. (d) Marshall, A. G.; Hendrickson, C. L.; Jackson, G. S. *Mass Spectrom. Rev.* **1998**, *17*, 1.

(4) Arshadi, R.; Yamdagni, R.; Kebarle, P. *J. Phys. Chem.* **1970**, *74*, 1475–1482.

(5) Meot-Ner (Mautner), M. *Chem. Rev.* **2005**, *105*, 213–284.

(6) Ayotte, P.; Bailey, C. G.; Johnson, M. A. *J. Phys. Chem. A* **1998**, *102*, 3067–3071.

(7) (a) Gatev, G. G.; Zhong, M.; Brauman, J. I. *J. Phys. Org. Chem.* **1997**, *10*, 531–536. (b) Bradforth, S. E.; Arnold, D. W.; Metz, R. B.; Weaver, A.; Neumark, D. M. *J. Phys. Chem.* **1991**, *95*, 8066–8078.

(8) (a) Peiris, D. M.; Riveros, J. M.; Eyler, J. R. *Int. J. Mass. Spectrom. Ion Processes* **1996**, *159*, 169–183. (b) Weiser, P. S.; Wild, D. A.; Bieske, E. J. *Chem. Phys. Lett.* **1999**, *299*, 303–308. (c) Weiser, P. S.; Wild, D. A.; Bieske, E. J. *J. Chem. Phys.* **1999**, *110*, 9443–9449.

(9) Such as cyclopentadienide anion: Meot-Ner (Mautner), M. *J. Am. Chem. Soc.* **1988**, *110*, 3858.

(10) (a) Mustanir, Matsuoka, M.; Mishima, M.; Koch, H. *Bull. Chem. Soc. Jpn.* **2006**, *79*, 1118–1125. (b) Chabinyc, M. L.; Brauman, J. I. *J. Am. Chem. Soc.* **2000**, *122*, 5371–5378. (c) Chabinyc, M. L.; Brauman, J. I. *J. Am. Chem. Soc.* **1999**, *103*, 9163–9166.

(11) Meot-Ner (Mautner), M.; Cybulski, S. M.; Scheiner, S.; Liebman, J. F *J. Phys. Chem.* **1988**, *92*, 2738–45.

(12) Mishima, M.; Matsuoka, M.; Lei, Y. X.; Rappoport, Z. *J. Org. Chem.* **2004**, *69*, 5347–65.

(13) (a) Wincel, H. *Int. J. Mass Spectrom.* **2003**, *226*, 341. (b) Sieck, L. W. *J. Phys. Chem.* **1985**, *89*, 5552. (c) Larson, J. W.; McMahon, T. B. *J. Am. Chem. Soc.* **1984**, *106*, 517. (d) Larson, J. W.; McMahon, T. B. *J. Am. Chem. Soc.* **1983**, *105*, 2945. (e) French, M. A.; Ikuta, S.; Kebarle, P. *Can. J. Chem.* **1982**, *60*, 1907.

(14) Andreades, S. *J. Am. Chem. Soc.* **1964**, *86*, 2003–10.

(15) (a) Sleigh, J. H.; Stephens, R.; Tatlow, J. C. *J. Chem Soc., Chem. Commun.* **1979**, *921*, 2. (b) Sleigh, J. H.; Stephens, R.; Tatlow, J. C. *J. Fluorine Chem.* **1980**, *15*, 411–22.

(16) (a) Koppel, I. A.; Pihl, V.; Koppel, I.; Anvia, F.; Taft, R. W. *J. Am. Chem. Soc.* **1994**, *116*, 8654–8657. (b) Koppel, I. A.; Taft, R. W.; Anvia, F.; Zhu, S.-Z.; Hu, L.-Q.; Sung, K.-S.; DesMarteau, D. D.; Yagupolskii, L. M.; Yagupolskii, Y. L.; Ignat'ev, N. V.; Kondratenko, N. V.; Volkonskii, A. Y.; Vlasov, V. M.; Notario, R.; Maria, P.-C. *J. Am. Chem. Soc.* **1994**, *116*, 3047–3057.

(17) Borodin, P. M.; Golubev, V. S.; Denisov, G. S.; Safarov, N. A. *Vestn. Leningr. Univ., Ser. 4* **1978**, *1*, 66–68; CA 89:23575.

(18) Chabinyc, M. L.; Brauman, J. I. *J. Am. Chem. Soc.* **2000**, *122*, 8739–8745.

(19) Chabinyc, M. L.; Brauman, J. I. *J. Am. Chem. Soc.* **1998**, *120*, 10863–10870.

(20) Larson, J. W.; McMahon, T. B. *J. Am. Chem. Soc.* **1984**, *106*, 517–521.

(21) Bartmess, J. E. Negative Ion Energetics Data. In *NIST Standard Reference Database Number 69*; Linstrom, P. J., Mallard, W. G., Eds.; National Institute of Standards and Technology (NIST): Gaithersburg, MD, 2003; available at http://webbook.nist.gov.

(22) Slater, C. D. *J. Org. Chem.* **1981**, *46*, 2173–75.

(23) Neutral fluorinated alkanes are known to be weak hydrogen-bond acceptors. See, for example: (a) Ouvrard, C.; Berthelot, M.; Laurence, C *J. Phys. Org. Chem.* **2001**, *14*, 804–810. (b) Ouvrard, C.; Berthelot, M.; Laurence, C. *J. Chem. Soc., Perkin Trans. 2* **1999**, *1357*, 1362.

(24) Laukien, F. H.; Allemann, M.; Bischofberger, P.; Grossmann, P.; Kellerhals, P.; Kopfel, P. In *Fourier Transform Mass Spectrometry: Evolution, Innovation and Applications*; Buchanan, M. V., Ed.; ACS Symposium Series; American Chemical Society: Washington, DC, 1987; Vol. 359, Chapter 5.

(25) (a) Dávalos, J. Z.; Herrero, R.; Quintanilla, E.; Jiménez, P.; Gal, J.-F.; Maria, P.-C.; Abboud, J.-L. M. *Chem.−Eur. J.* **2006**, *12*, 5505–5513. (b) Dávalos, J. Z.; Herrero, R.; Abboud, J.-L. M.; Mó, O.; Yáñez, M. *Angew. Chem., Int. Ed.* **2007**, *46*, 381–5. (c) R. Herrero, R.; Dávalos, J. Z.; Abboud, J.-L. M.; Alkorta, I.; Koppel, I. A.; Koppel, I.; Sonoda, T.; Mishima, M *Int. J. Mass. Spectrom.* **2007**, *267*, 302–307.

(26) Becke, A. D. *J. Chem. Phys.* **1993**, *98*, 1372–1377.

(27) (a) Møller, C.; Plesset, M. S. *Phys. Rev.* **1934**, *46*, 618–622. (b) Leininger, M. L.; Allen, W. D.; Schaefer, H. F., III. *J. Chem. Phys.* **2000**, *112* (21), 9213–9222.

(28) Davidson, E. R.; Feller, D. *Chem. Rev.* **1986**, *86* (4), 681–696.

(29) Frisch, M. J.; Trucks, G. W.; Schlegel, H. B.; Scuseria, G. E.; Robb, M. A.; Cheeseman, J. R.; Montgomery, J. A., Jr.; Vreven, T.; Kudin, K. N.; Burant, J. C.; Millam, J. M.; Iyengar, S. S.; Tomasi, J.; Barone, V.; Mennucci, B.; Cossi, M.; Scalmani, G.; Rega, N.; Petersson, G. A.; Nakatsuji, H.; Hada, M.; Ehara, M.; Toyota, K.; Fukuda, R.; Hasegawa, J.; Ishida, M.; Nakajima, T.; Honda, Y.; Kitao, O.; Nakai, H.; Klene, M.; Li, X.; Knox, J. E.; Hratchian, H. P.; Cross, J. B.; Bakken, V.; Adamo, C.; Jaramillo, J.; Gomperts, R.; Stratmann, R. E.; Yazyev, O.; Austin, A. J.; Cammi, R.; Pomelli, C.; Ochterski, J. W.; Ayala, P. Y.; Morokuma, K.; Voth, G. A.; Salvador, P.; Dannenberg, J. J.; Zakrzewski, V. G.; Dapprich, S.; Daniels, A. D.; Strain, M. C.; Farkas, O.; Malick, D. K.; Rabuck, A. D.; Raghavachari, K.; Foresman, J. B.; Ortiz, J. V.; Cui, Q.; Baboul, A. G.; Clifford, S.; Cioslowski, J.; Stefanov, B. B.; Liu, G.; Liashenko, A.; Piskorz, P.; Komaromi, I.; Martin, R. L.; Fox, D. J.; Keith, T.; Al-Laham, M. A.; Peng, C. Y.; Nanayakkara, A.; Challacombe, M.; Gill, P. M. W.; Johnson, B.; Chen, W.; Wong, M. W.; Gonzalez, C.; Pople, J. A. *Gaussian 03*, revision B.05; Gaussian, Inc.: Pittsburgh, PA, 2003.

(30) Reed, A. E.; Curtiss, L. A.; Weinhold, F. *Chem. Rev.* **1988**, *88*, 899–926.

(31) NBO, version 3.1: Glendening, E. D.; Reed, A. E.; Carpenter, J. E.; Weinhold, F., as included in ref 29.

(32) (a) In solution in tetraglyme: Bayliff, A. E.; Bryce, M. R.; Chambers, R. D.; Matthews, R. S. *J. Chem. Soc., Chem. Commun.* **1985**, *101*, 8–1019. (b) Boys, S. F.; Bernardi, F. *Mol. Phys.* **1970**, *19*, 553–566.

(33) Burk, P.; Koppel, I. A.; Koppel, I.; Yagupolskii, L.; Taft, R. W. *J. Comput. Chem.* **1996**, *17*, 30–41.

(34) The scaled PM3 method involved full geometry optimization at the SCF level using a double-ζ-quality basis set augmented with polarization and diffuse functions: Dixon, D. A.; Fukunaga, T.; Smart, B. E. *J. Am. Chem. Soc.* **1986**, *108*, 4027–4031.

(35) (a) Stølevik, R.; Thom, E. *Acta Chem. Scand.* **1971**, *25*, 3205–3212. (b) Munrow, M. R.; Subramanian, R.; Minei, A. J.; Antic, D.; MacLeod, M. K.; Michl, J.; Crespo, R.; Piqueras, M. C.; Izuha, M.; Ito, T.; Tatamitani, Y.; Yamanou, K.; Ogata, T.; Novick, S. E. *J. Mol. Spectrosc.* **2007**, *242* (2), 129–139.

(36) Wiberg, K. B. *Tetrahedron* **1968**, *24*, 1083–1096.

(37) Kirkpatrick, S.; Gelatt, C. D.; Vecchi, M. P., Jr. *Science* **1983**, *220*, 671–680.

(38) Average of the values given in ref 20.

(39) (a) Bader, R. W. F.; MacDougall, P. J.; Lau, C. D. H. *J. Am. Chem. Soc.* **1984**, *106*, 1594–1605. (b) Bader, R. W. F. *Atoms in Molecules—A Quantum Theory*; Oxford University Press: New York, 1990.

(40) For a discussion on AIM hydrogen-bond analysis, see, for example: Carroll, M. T.; Bader, R. W. F. *Mol. Phys.* **1988**, *63*, 387–405.

(41) Ikuta, S.; Saitoh, T.; Nomura, O. *J. Chem. Phys.* **1989**, *91*, 3539–3548. This work reports a computed value for $\Delta_r G^0_m(4)$ of −16.5 kcal mol^{-1}.

(42) Kar, T.; Sánchez Marcos, E. *Chem. Phys. Lett.* **1992**, *192*, 14–19.

(43) Parr, R. G.; Ayers, P. W.; Nalewajski, R. F *J. Phys. Chem. A* **2005**, *109* (17), 3957–3959.

(44) Batsanov, S. S. *J. Mol. Struct. (THEOCHEM)* **1999**, *468*, 151–159.

(45) Alkorta, I.; Elguero, *J. Struct. Chem.* **2004**, *15*, 117–120.

(46) Alkorta, I.; Elguero, J. *J. Chem. Phys.* **2002**, *117*, 6463–6468.

(47) Peralta, J. E.; Contreras, R. H.; Snyder, J. P. *J. Chem. Soc., Chem. Commun.* **2000**, 2025–2026.

JP811057M